EurJIC
European Journal of Inorganic Chemistry

Chemistry Europe
European Chemical Societies Publishing

Accepted Article

Title: Controlled Supramolecular Assembly of Gold (III) Amphiphiles in Aqueous Media

Authors: Jia-Jun Jiang, Anson Kwok-Hei Chau, Man-Kin Wong, and Franco King Chi Leung

To be cited as: *Eur. J. Inorg. Chem.* **2022**, e202200281

Link to VoR: https://doi.org/10.1002/ejic.202200281

WILEY-VCH

WILEY-VCH

RESEARCH ARTICLE

Controlled Supramolecular Assembly of Gold (III) Amphiphiles in Aqueous Media

Jia-Jun Jiang, Anson Kwok-Hei Chau, Man-Kin Wong,* and Franco King-Chi Leung*

[a] J.-J. Jiang, A. K.-H. Chau, Dr. M.-K. Wong, Dr. F. K.-C. Leung
State Key Laboratory of Chemical Biology and Drug Discovery
Department of Applied Biology and Chemical Technology
The Hong Kong Polytechnic University
Hung Hom (Hong Kong)
E-mail: mankin.wong@polyu.edu.hk; kingchifranco.leung@polyu.edu.hk
Home Pages: https://www.polyu.edu.hk/abct/people/academic-staff/dr-wong-man-kin/; http://francokingchileung.com/

Supporting information for this article is given via a link at the end of the document.

Abstract: Supramolecular assemblies of gold complex-based amphiphiles in aqueous media are highly structural sensitive to external environments, providing an attractive prospect for its application in soft functional materials. Notably, the development of a supramolecular assembly transformation of gold (III) amphiphile directly controlled by counterion exchange is of fundamental importance for exerting the full potential of dynamic supramolecular assembly by external stimuli. Here we present a reversible supramolecular assembly of gold (III) amphiphiles controlled by counterions in aqueous media and their co-assembly with gold nanoparticles.

Introduction

Controlled supramolecular assembly of biomolecules into functional structures, such as cell membranes and cytoskeleton filaments, serves as key roles in precise and proper functioning of biological processes.[1–3] A variety of non-covalent interactions among basic assembled units provides a fundamental toolbox for designing artificial and synthetic supramolecular assembling systems.[4,5] The structural diversity, dynamic nature and responsiveness to stimulations of synthetic supramolecular assemblies and polymers in aqueous media allows the realization of biomimetic functions with non-biocompatible stimulations or energy sources as inputs.[4–7] Recent advancements in supramolecular chemistry and soft functional materials have rendered a series of supramolecular assemblies, mesogens, polymeric liquid crystals, polymeric elastomers, and hybrid composites the responsiveness to external stimulations in aqueous media, including heat, pH, ions, light.[8–10] Amphiphile is one of the key candidates in the design of synthetic organic molecules with high functional tunability and aqueous solubility, as amphiphilic structures interact differently with the solvent/water.[4,11] Compared with the extensively investigated supramolecular assemblies and co-assemblies of organic amphiphiles,[5] metal-ligand amphiphiles serve as a promising alternative for their structural diversity and versatility of ligand modifications via simpler synthetic strategies.[12–16] The tunability of metal-ligand amphiphile design allows a delicate control in structure and intermolecular interactions with various noncovalent interactions.[12,16]

Gold (I) and gold (III) complexes, known for their wide range of applications in catalysis,[17–19] optoelectronic materials[20,21] and bioconjugation methodologies,[22–24] have been extensively developed due to their unique luminescence properties and aqueous stability. Pioneering amphiphilic molecular design of cyclometalated gold (III),[25–29] a system, featured with polyethene glycol (PEG), has provided micellar assemblies with good biocompatibility and aqueous solubility in exhibiting activity towards *in vitro* phototoxicity, reported by Che.[30] In 2018, Besenius and co-workers reported gold (I) metallo-amphiphile with a kinetically controlled stepwise nanofibre assembly in buffered aqueous solution.[31] Later, a series of charged cyclometalated gold (III) complexes were reported by Che, providing kinetically controlled supramolecular assemblies in ACN/water media.[32] Yam and co-workers have further demonstrated their charged cyclometalated gold (III) amphiphile designs with intrinsic multiple responsiveness and gel-sol process in organic media.[33] The reported gold amphiphiles showed high structural sensitivity to minor molecular structure change, *i.e.*, a counterion effect on the packing parameters change, induced supramolecular structural transformations.[30,32,33] However, a reversibly controlled supramolecular assembly transformation of cyclometalated gold (III) amphiphiles induced by direct addition of reagents, *i.e.*, counterion exchange, in aqueous media and a supramolecular co-assembly of cyclometalated gold (III) amphiphiles, to best of our knowledge, are remained largely unexplored.

Previously, we have developed a class of gold (III) complexes for versatile applications ranging from catalysis[34,35] to bioconjugation methodologies.[36–38] These cyclometalated gold (III) complexes provide a synthetic toolbox for chemoselective modifications of biomolecules in aqueous media. Furthermore, we have demonstrated that the photoresponsive molecular amphiphiles, such as motor amphiphiles, can be potentially developed to supramolecular actuators and stimuli-responsive supramolecular assemblies in aqueous media.[39–41] Herein, we have designed and synthesised a new class of C^N cyclometalated gold (III) amphiphiles (GA), connected to a quaternary ammonium ion with an alkyl-linker to cyclometalated gold (III) motif. Maximised molecular phase separation of GA gives a large aspect ratio of supramolecular assembly with excellent aqueous solubility and stability. It is noted that no implementation of large molecular weight PEG and co-solvents are required to exhibit an excellent aqueous solubility of GA. Packing parameters of GAs can be finely adjusted by the counterion substitution, such as sodium halides and tosylate, resulting in a reversibly controlled supramolecular transformation (Scheme 1). Supramolecular assembly of GA can also serve as a

template for controlled gold nanoparticles (AuNP) growth, allowing supramolecular co-assembly of GA with AuNP. The co-assembly of GA/AuNP lay the foundation in developing next generation of chiral-templated AuNP by fine adjustment of chiral environment of GA. By elucidating the supramolecular assembly transformation conditions, this could open up new prospects toward the development of externally stimuli-controlled soft functional materials.

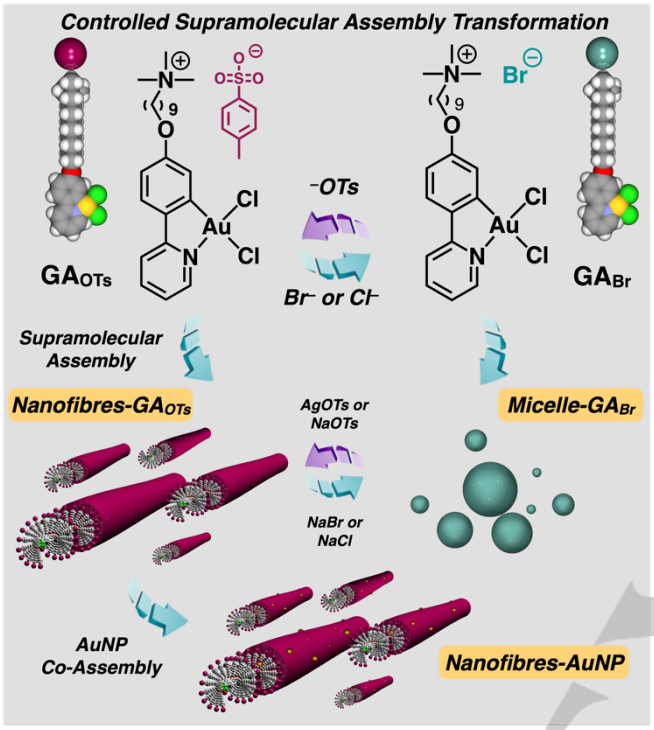

Scheme 1. Schematic illustration of supramolecular assemblies and co-assembly with AuNP of GAs and the corresponding supramolecular transformations.

Results and Discussion

Design and Synthesis of GA$_{OTs}$ and GA$_{Br}$

Gold amphiphiles were designed with C^N cyclometalated gold (III) complex core attached with a quaternary ammonium ion motif by a nonyl-linker with either a tosylate group or a bromide as the counter anion (Scheme 1). The synthetic routes for gold (III) amphiphiles **GA$_{OTs}$** and **GA$_{Br}$** are shown in Scheme 2. Firstly, ligand 4-(Pyridin-2-yl)phenol was tethered with different nonyl-linkers, respectively, affording compound **1** and **5**. Gold (III) complexes **4** and **7** were synthesised according to reported metalation methodologies. Dioxane is adopted as the solvent in replacement of ethanol in the synthesis of organomercury compound **6**, preventing ethoxylation of bromo-substituted nonyl-linker. The nucleophilic substitutions of gold complexes **4** and **7** with trimethylamine afforded gold (III) amphiphiles, **GA$_{OTs}$** and **GA$_{Br}$**, respectively. The structural characterisation of **GA$_{OTs}$**, **GA$_{Br}$**, and their precursors are summarised (Figure S11–S26).

A freshly prepared aqueous solution of **GA$_{OTs}$** (6.3 mM) was heated to 50 °C for 5 min and slowly cooled to 20 °C over 30 min, *i.e.*, thermal annealing process. The solution was diluted into a range of concentrations from 0.01 to 2.0 mM for the determination of the critical aggregation concentration (CAC) by using a Nile Red fluorescence assay (NRFA), which probes the internal hydrophobicity of assemblies. The CAC of **GA$_{OTs}$** was determined as 0.19 mM (Figure S1). An aqueous solution of **GA$_{OTs}$** (200 μM) was heated to 50 °C and slowly cooled to 20 °C at a rate of 1.0 °C/min, studied by UV-vis absorption spectroscopy (Figure 1a, red-line). The absorption maximum at 348 nm of **GA$_{OTs}$** decreased in the cooling process with a formation of bathochromic-shifted band appearing at 355 nm (Figure 1a, black-line), indicating the formation of supramolecular assembly of **GA$_{OTs}$**. A thermal annealed aqueous solution of **GA$_{OTs}$** (6.3 mM) was examined with negative-stained transmission electron microscopy (TEM), revealing nanofibres with hundreds of nanometres to micrometres in length and 5–6 nm in diameter (Figure 1b). It is noted that the nanofibres of **GA$_{OTs}$** are racemic helical nanofibrillar structures in considering its diameter with minimised surface charge. No significant spectral shift is observed in UV-vis absorption spectra upon the increase in concentration of **GA$_{OTs}$** from 10 μM to 500 μM (Figure S2), suggesting no supramolecular transformation at increased concentration.

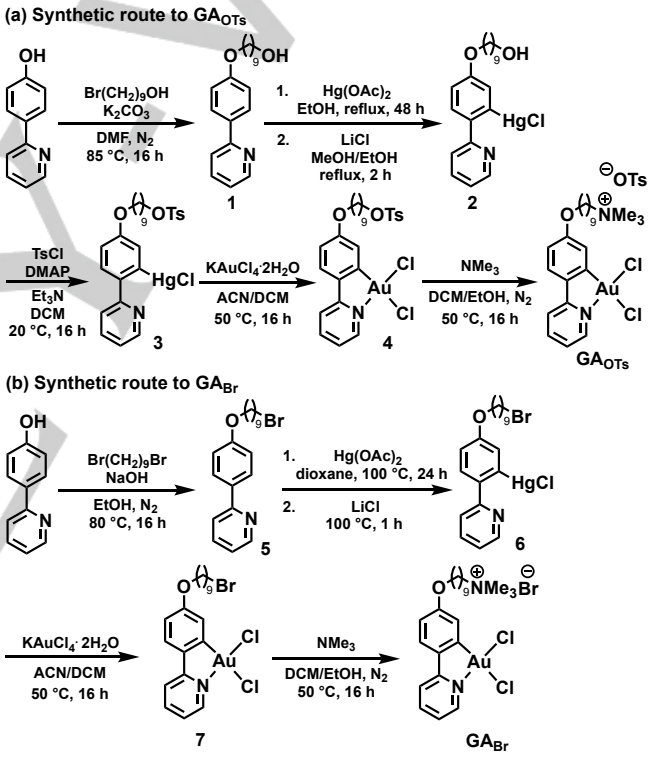

Scheme 2. Synthetic route of gold (III) amphiphiles (a) **GA$_{OTs}$** (b) **GA$_{Br}$**.

Supramolecular Assembly and Co-Assembly of GA$_{OTs}$ in Aqueous Media

A PBS buffer (pH 7.4, Figure 2a) and a Tris buffer (pH 7.0, 25 mM, Figure. S3) solution of **GA$_{OTs}$** (6.3 mM) were prepared by identical thermal annealing process to give essentially identical supramolecular nanofibre structure to that of the obtained aqueous solution of **GA$_{OTs}$** (Figure 1b). The results indicate that the nanofibres of **GA$_{OTs}$** show excellent stability at pH 7. An aqueous mixture solution (without buffer) of **GA$_{OTs}$** (6.3 mM) and $KAuCl_4$ (63 μM) afforded irregular supramolecular assembly in TEM image (Figure S4a), possibly due to the pH variation upon $KAuCl_4$ addition. In contrast, nanofibres were revealed in both PBS buffer mixture (Figure 2b) and Tris buffer mixture (Figure S4b) solutions of **GA$_{OTs}$** (6.3 mM) and $KAuCl_4$ (63 μM) after

incubated at 20 °C for 16 h. It is noted that fewer nanofibres were found in the Tris buffer mixture (Figure S4b). Furthermore, the nanofibres of a PBS buffer solution of **GA_{OTs}** (6.3 mM) remained stable even in the presence of a higher concentration of $KAuCl_4$ (3.2 mM, Figure S5). The results indicate that the $AuCl_4^-$ counterion effect to the supramolecular structure of **GA_{OTs}** is minimised in PBS buffer.

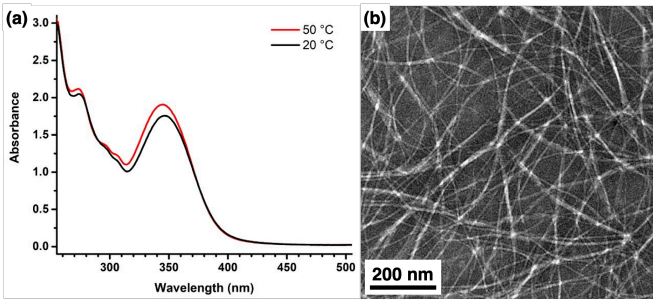

Figure 1. (a) UV-vis absorption spectra of **GA_{OTs}** (200 μM) was cooled from 50 °C (red-line) to 20 °C (black-line) at a rate of 1.0 °C/min. (b) TEM image of aqueous solution of **GA_{OTs}** (6.3 mM) after thermal annealing.

The outstanding stability of **GA_{OTs}** nanofibres can be potentially applied as a template for gold nanoparticles (AuNP) growth. After the incubation of **GA_{OTs}** (3.2 mM) with $KAuCl_4$ (158 μM) at 20 °C for 16 h, a reducing agent tetrakis-(hydroxymethyl) phosphonium chloride (THPC, 118 μM) was added for further incubation at 20 °C for 3 h. TEM image of the solution showed that the **GA_{OTs}** nanofibres remained stable with AuNP (2–3 nm in diameter) distributed mainly onto the surface of **GA_{OTs}** nanofibres (Figure 2c). AuNP randomly decorated onto the surface of nanofibres is possibly due to the electrostatic interaction between $AuCl_4^-$ and quaternary ammonium ion of **GA_{OTs}**, allowing AuNP nucleation and growth onto surface of nanofibres. However, a higher concentrated mixture of $KAuCl_4$ (1.58 mM) and THPC (1.18 mM) in **GA_{OTs}** (3.2 mM) induced the disassembly of nanofibres into micellar structures with an uncontrolled size of AuNP (Figure 2d). The results reveal that slow growth of AuNP with a lower concentration of THPC are crucial to afford AuNP with controlled size and stable co-assembly of AuNP with **GA_{OTs}** nanofibres. In addition, another reducing agent sodium ascorbate (SA) was incubated with **GA_{OTs}** nanofibres and $KAuCl_4$, but the size of AuNP cannot be controlled (Figure S6). Although the origin of AuNP cannot be traced, the results demonstrated that **GA_{OTs}** can serve as a template for AuNP growth, affording co-assembly of **GA_{OTs}** nanofibres decorated with AuNP.

Supramolecular Assembly Transformations of GA_{OTs} and GA_{Br}

Furthermore, an aqueous solution (without buffer) **GA_{Br}** was heated to 50 °C for 5 min and slowly cooled to 20 °C to give a transparent pale-yellow solution. The CAC of **GA_{Br}** was determined as 0.12 mM (Figure S7) by NRFA. A thermal annealed aqueous solution of **GA_{Br}** (7.1 mM) was measured with TEM to reveal a micellar structure with 10–50 nm in diameter (Figure 3a–3b). The size of **GA_{Br}** micellar structures was further confirmed with dynamic light scattering (DLS), showing size distribution 30–60 nm (Figure S8). By changing the counter anion from inorganic anion bromide to organic anion tosylate, the supramolecular structure of GA is transformed from micellar structures ($P \leq 1/3$) to nanofibres ($1/3 < P \leq 1/2$), suggesting the packing parameters tuning with counter anions. To control the supramolecular transformation of GA, a thermal annealed aqueous solution of **GA_{Br}** (7.1 mM) was added with AgOTs (7.1 mM) for further incubation at 20 °C for 15 min to afford supramolecular nanofibres (Figure 3b–3c), which is essentially identical to that of observed in the aqueous solution of **GA_{OTs}** (Figure 1b). Some dark nanoparticles were also found in the TEM image and its major composition was confirmed as silver bromide by TEM-energy-dispersive X-ray spectroscopy (TEM-EDS) (Figure S9). The silver bromide nanoparticle is the side product after the counter exchange of **GA_{Br}** (7.1 mM) was added with AgOTs.

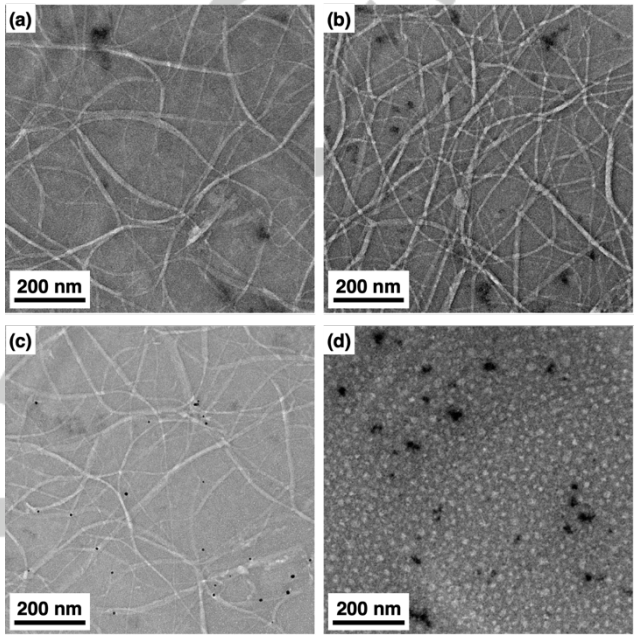

Figure 2. TEM images of (a) a PBS buffer (pH 7.4) mixture solution of **GA_{OTs}** (6.3 mM) after thermal annealing and (b) with $KAuCl_4$ (63 μM) after incubated at 20 °C for 16 h. TEM images of a PBS buffer (pH 7.4) mixture solution of **GA_{OTs}** (3.2 mM) (c) with $KAuCl_4$ (158 μM) and THPC (118 μM) and (d) with $KAuCl_4$ (1.58 mM) and THPC (1.18 mM).

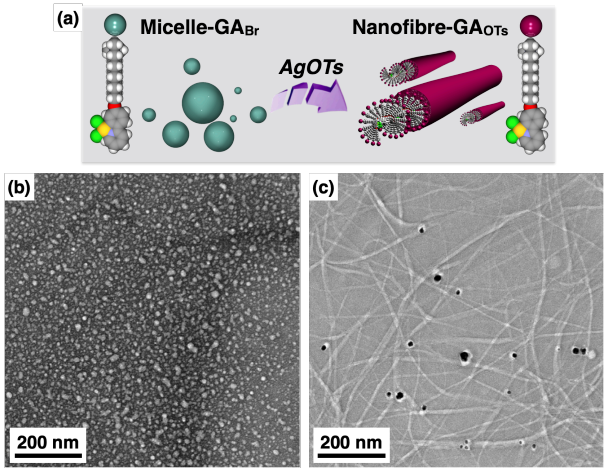

Figure 3. (a) Schematic illustration for counterion exchange of **GA_{Br}** with AgOTs. TEM images of (b) a thermal annealed aqueous solution of **GA_{Br}** (7.1 mM) and (c) after addition of AgOTs (7.1 mM) incubated at 20 °C for 15 min.

Supramolecular assembly transformation from nanofibres ($1/3 < P \leq 1/2$) to micellar structures ($P \leq 1/3$) was also achieved by counterion exchange from organic anion tosylate to inorganic halide anions (chloride and bromide) (Figure 4a). A thermal

annealed aqueous solution of **GA_{OTs}** (6.3 mM) was added with solutions of sodium bromide or sodium chloride (12.6 mM), respectively, which two equivalent of sodium halides are required to substitute strongly bound OTs^- with the charged headgroup of **GA_{OTs}**.[42] The mixture solution was treated with a second thermal annealing process. For the thermal annealed mixture solution of **GA_{OTs}** (6.3 mM) with NaBr (12.6 mM), TEM results revealed a supramolecular transformation from nanofibres to micellar structures (Figure 4b), which is essentially identical to that of observed in the aqueous solution of **GA_{Br}** (Figure 3a). The reversible supramolecular transformation of GA can only be performed in one cycle, as excess ions acumination will significantly change the resulting assembly structures. For the second thermal annealed mixture solution of **GA_{OTs}** (6.3 mM) with NaCl (12.6 mM), similar micellar structures were observed in TEM image (Figure 4c). It is noted that the micellar structures, prepared from **GA_{OTs}** with NaBr and NaCl, featured with diameter 10–50 nm (Figure S10). The results indicate that supramolecular assembly transformation of GA can be controlled by the direct addition of counterion without additional organic synthesis. Nevertheless, sodium iodide was not studied by TEM due to the sensitivity of GA to reductive iodide ion. As a control experiment, a thermal annealed aqueous solution of **GA_{OTs}** (6.3 mM) was treated with a second thermal annealing process in the absence of sodium halide, showing nanofibres remained (Figure 4d). Furthermore, a thermal annealed aqueous solution of **GA_{Br}** (6.3 mM) was added with solution of sodium tosylate (12.6 mM) and annealed, providing nanofibres (Figure 4e) essentially identical to that of observed in Figure 1b. The obtained results clearly indicated that reversible supramolecular transformations of GA can be achieved by counterion exchange with sodium salts.

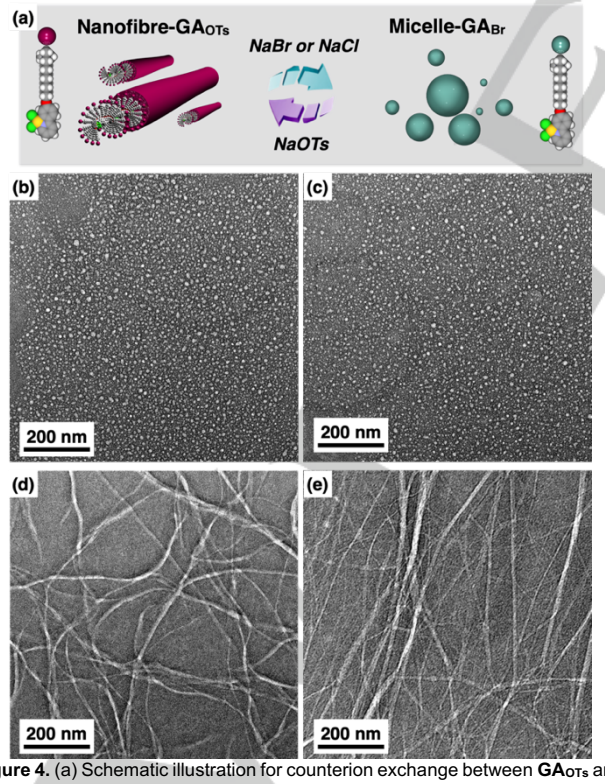

Figure 4. (a) Schematic illustration for counterion exchange between **GA_{OTs}** and **GA_{Br}** with sodium salts. TEM images of (b) a mixture solution of **GA_{OTs}** (6.3 mM) and NaBr (12.6 mM), (c) a mixture solution of **GA_{OTs}** (6.3 mM) and NaCl (12.6 mM), and (d) an aqueous solution of **GA_{OTs}** (6.3 mM) were thermally annealed at 50 °C and cooled down to 20 °C. TEM image of (e) a mixture solution of **GA_{Br}** (6.3 mM) and NaOTs (12.6 mM) was thermally annealed at 50 °C and cooled down to 20 °C.

Conclusion

Gold (III) amphiphiles, which respond reversibly to counterion exchange and to co-assemble with AuNP in a controllable manner, were designed and clearly demonstrated. Nanofibres of **GA_{OTs}** were confirmed by TEM and NRFA. **GA_{OTs}** can serve as a template for AuNP growth. Reversible supramolecular assembly transformation of **GA_{OTs}** between nanofibres and micelles was demonstrated. The current approach might open up new prospects to produce stimuli controlled supramolecular assembly of gold amphiphiles.

Experimental Section

Preparation of Gold (III) Amphiphile Solutions with Thermal Annealing Process:

GA_{OTs} aqueous solution (12.6 mM, 1.0 wt.%): Gold (III) amphiphile **GA_{OTs}** (1.0 mg) was dissolved in Milli-Q water (99.0 μL). The obtained solution was heated at 50 °C for 5 min, and slowly cool down to 20 °C over 30 min, obtaining an aqueous solution of **GA_{OTs}** (12.6 mM, 1.0 wt.%). The obtained aqueous solution of **GA_{OTs}** was diluted to 6.3 mM for analysis by transmission electron microscopy (TEM, Figure 1b). 3).

Buffered solutions of GA_{OTs} (12.6 mM, 1.0 wt.%): Gold (III) amphiphile **GA_{OTs}** (1.0 mg) was dissolved in a PBS buffer solution (pH 7.4, 1x dilution, 99.0 μL) or a Tris buffer (pH 7.0, 25 mM, 99.0 μL). The obtained solutions were heated at 50 °C for 5 min, and slowly cool down to 20 °C over 30 min, respectively obtaining the PBS buffer and Tris buffer solutions of **GA_{OTs}** (12.6 mM, 1.0 wt.%). The obtained buffered solutions of **GA_{OTs}** were diluted to 6.3 mM for analysis by TEM (Figure 2a and Figure S3).

GA_{Br} aqueous solution (14.2 mM, 1.0 wt.%): Gold (III) amphiphile **GA_{Br}** (1.0 mg) was dissolved in Milli-Q water (99.0 μL). The obtained solution was heated at 50 °C for 5 min, and slowly cool down to 20 °C over 30 min, obtaining an aqueous solution of **GA_{Br}** (14.2 mM, 1.0 wt.%). The obtained aqueous solution of **GA_{Br}** was diluted to 7.1 mM for analysis by TEM (Figure 3a).

Incubation of GA_{OTs} Nanofibres with $KAuCl_4$: As a general procedure, a solution of **GA_{OTs}** after thermal annealing process and a stock solution of $KAuCl_4$ (1.0 mM or 10.0 mM) were combined and diluted with Milli-Q water or a buffer solution. The mixture was incubated at 20 °C for 16 h, obtaining a mixture solution of **GA_{OTs}** (final concentration, 6.3 mM) and $KAuCl_4$ (different final concentrations). The mixture solutions were analysed by TEM (Figure 2b, Figure S4, and Figure S5).

Gold Nanoparticles (AuNP) Growth on GA_{OTs} Nanofibres: As a general procedure, a PBS buffered (pH 7.4, 1x dilution) solution of a reducing agent (tetrakis-(hydroxymethyl) phosphonium chloride or sodium ascorbate) was added into a PBS buffered (pH 7.4, 1x dilution) mixture solution of GA_{OTs} (6.3 mM) and $KAuCl_4$ (prepared from the procedure above). The resulting mixture was incubated at 20 °C for 3 h, obtaining a mixture solution of GA_{OTs} (3.2 mM) with $KAuCl_4$ and reducing agent. The obtained mixture solutions were analysed by TEM (Figure 2c and Figure S6).

Incubation of GA_{Br} with AgOTs for Counter Anion Controlled Supramolecular Transformation: A thermal annealed aqueous solution of **GA_{Br}** (14.2 mM, 10 μL) was added with an aqueous solution of AgOTs (20 mM, 7.1 μL) and Milli-Q water (2.9 μL). The mixture solution was incubated at 20 °C for 15 min. The resulting turbid solution was analysed by TEM (Figure 3b).

Incubation of GA_{OTs} with Sodium Halide for Counter Anion Controlled Supramolecular Transformation: A thermal annealed aqueous solution

of GA_{OTs} (12.6 mM, 20 μL) was added with an aqueous solution of sodium halide (25.2 mM, 20 μL). The obtained solution was incubated at 50 °C for 5 min, and slowly cool down from 50 °C to 20 °C over 30 min. The resulting solutions were analysed by TEM (Figure 4a, 4b). Milli-Q water was used in replacement of sodium halide solution for control experiment (Figure 4c).

Incubation of GA_{Br} with Sodium Tosylate for Counter Anion Controlled Supramolecular Transformation: A thermal annealed aqueous solution of GA_{Br} (14.2 mM, 20 μL) was added with an aqueous solution of sodium tosylate (28.4 mM, 20 μL). The obtained solution was incubated at 50 °C for 5 min, and slowly cool down from 50 °C to 20 °C over 30 min. The resulting solutions were analysed by TEM (Figure 4e).

Synthesis

Compound 1: 2-(4-Hydroxyphenyl)pyridine (1.0 g, 5.8 mmol), 9-bromononanol (1.56 g, 7.0 mmol) and K_2CO_3 (1.6 g, 12 mmol) were added to dimethylformamide (DMF, 10 mL) and heated under N_2 at 85 °C for 16 h. After the reaction completed, the resulting mixture was diluted with 50 mL ethyl acetate (EA), and then washed by deionized water (80 mL) for three times. The obtained organic phase was dried over anhydrous $MgSO_4$ and subjected to flash column chromatography (dichloromethane/EA = 3/1, R_f = 0.3) to obtain product **1** as a white solid (1.07 g, 3.4 mmol, 59% yield). ^{1}H NMR (400 MHz, $CDCl_3$) δ 8.64 (d, J = 4.7 Hz, 1H), 7.96 – 7.89 (m, 2H), 7.75 – 7.63 (m, 2H), 7.20 – 7.12 (m, 1H), 7.03 – 6.94 (m, 2H), 4.01 (t, J = 6.5 Hz, 2H), 3.63 (t, J = 6.7 Hz, 2H), 1.86 – 1.74 (m, 2H), 1.61 – 1.51 (m, 2H), 1.51 – 1.42 (m, 2H), 1.40 – 1.29 (m, 8H). ^{13}C NMR (101 MHz, $CDCl_3$) δ 160.0, 157.2, 149.5, 136.7, 131.8, 128.1, 121.4, 119.8, 114.7, 68.1, 63.1, 32.8, 29.5, 29.3, 29.3, 29.2, 26.0, 25.7. HR-MS (ESI+) calculated for $C_{20}H_{27}NO_2$ $[M+H]^+$ 314.2115 found 314.2135.

Compound 2: Compound **2** was synthesized according to a published method.[43] Compound **1** (673 mg, 2.15 mmol) and $Hg(OAc)_2$ (754 mg, 2.37 mmol) were suspended in ethanol (EtOH, 10 mL) and refluxed for 48 h. Then, methanol solution (MeOH, 5 mL) of LiCl (201 mg, 4.73 mmol) was added to the reaction mixture. After addition, the reaction mixture was refluxed for further 2 h. After the reaction completed, the mixture was evaporated under vacuum and then subjected to flash column chromatography (*n*-hexane/dichloromethane = 1/3, R_f = 0.3) to afford compound **2** as a white solid (540 mg, 0.98 mmol, 46% yield). ^{1}H NMR (400 MHz, $CDCl_3$) δ 8.57 (d, J = 4.4 Hz, 1H), 7.96 (d, J = 8.8 Hz, 1H), 7.87 (d, J = 8.3 Hz, 1H), 7.82 – 7.73 (m, 1H), 7.33 – 7.25 (m, 1H), 7.09 (d, J = 2.6 Hz, 1H), 6.91 (dd, J = 8.7, 2.7 Hz, 1H), 4.01 (t, J = 6.5 Hz, 2H), 3.70 – 3.60 (m, 2H), 1.87 – 1.75 (m, 2H), 1.62 – 1.53 (m, 2H), 1.52 – 1.42 (m, 2H), 1.43 – 1.28 (m, 8H), 1.27 – 1.20 (m, 1H). ^{13}C NMR (101 MHz, $CDCl_3$) δ 160.3, 155.4, 149.4, 147.9, 138.1, 134.0, 127.8, 123.59, 122.6, 119.6, 114.8, 68.2, 63.1, 32.8, 29.5, 29.4, 29.3, 29.2, 26.0, 25.7. HR-MS (ESI+) calculated for $C_{20}H_{26}ClHgNO_2$ $[M+H]^+$ 550.1437 found 550.1420.

Compound 3: To a mixture of compound **2** (110 mg, 0.2 mmol), 4-dimethylaminopyridine (DMAP) (2.5 mg, 0.02 mmol) and triethylamine (Et_3N) (100 μL) in dichloromethane (DCM, 2 mL), *p*-toluenesulfonyl chloride (TsCl) (48 mg, 0.25 mmol) was added. The reaction mixture was stirred for 16 h at 20 °C. After the reaction completed, the mixture was washed with deionized water (2 mL), dried over anhydrous $MgSO_4$ and then subjected to flash column chromatography (*n*-hexane/DCM = 1/1, R_f = 0.6) to obtain compound **3** as a white solid (81 mg, 0.12 mmol, 58% yield). ^{1}H NMR (400 MHz, $CDCl_3$) δ 8.55 (d, J = 4.7 Hz, 1H), 7.95 (d, J = 8.7 Hz, 1H), 7.86 (d, J = 8.1 Hz, 1H), 7.82 – 7.72 (m, 3H), 7.34 (d, J = 8.0 Hz, 2H), 7.32 – 7.25 (m, 1H), 7.07 (d, J = 2.6 Hz, 1H), 6.90 (dd, J = 8.8, 2.7 Hz, 1H), 4.07 – 3.95 (m, 4H), 2.45 (s, 3H), 1.85 – 1.73 (m, 2H), 1.70 – 1.58 (m, 2H), 1.51 – 1.39 (m, 2H), 1.37 – 1.23 (m, 8H). ^{13}C NMR (101 MHz, $CDCl_3$) δ 160.2, 155.4, 149.4, 147.8, 144.7, 138.1, 133.9, 133.2, 129.8, 127.9, 123.6, 122.6, 119.6, 114.8, 70.7, 68.2, 29.3, 29.2, 29.2, 28.9, 28.8, 26.0, 25.3, 21.7. HR-MS (ESI+) calculated for $C_{27}H_{32}ClHgNO_4S$ $[M+H]^+$ 704.1525 found 704.1507.

Compound 4: Compound **4** was synthesized according to a published method.[44] Compound **3** (75 mg, 0.11 mmol) and $KAuCl_4{\cdot}2H_2O$ (53 mg, 0.13 mmol) were dissolved in a solvent mixture of acetonitrile/dichloromethane (ACN/DCM = 1/1) and heated for 16 h at 50 °C. The resulting solution was evaporated under vacuum. The resulting residue was suspended by DCM, and then filtered. The filtrate was concentrated by rotary evaporation and subjected to flash column chromatography (DCM, R_f = 0.6) to afford the crude product of tosylated cyclometallated gold (III) complex **4**. The crude product was recrystallized (MeOH/DCM = 10/1) to obtain the purified compound **4** as a yellow solid (62 mg, 0.084 mmol, 80% yield). ^{1}H NMR (400 MHz, CD_2Cl_2) δ 9.64 (d, J = 5.9 Hz, 1H), 8.14 – 8.01 (m, 1H), 7.83 – 7.70 (m, 3H), 7.61 – 7.48 (m, 2H), 7.46 – 7.32 (m, 3H), 6.93 (dd, J = 8.5, 2.3 Hz, 1H), 4.08 (t, J = 6.5 Hz, 2H), 4.01 (t, J = 6.5 Hz, 2H), 2.46 (s, 3H), 1.86 – 1.74 (m, 2H), 1.69 – 1.59 (m, 2H), 1.51 – 1.41 (m, 2H), 1.37 – 1.24 (m, 8H). Due to the low solubility, ^{13}C NMR spectrum of compound **4** cannot be obtained. HR-MS (ESI+) calculated for $C_{27}H_{32}AuCl_2NO_4S$ $[M+Na]^+$ 756.0987 found 756.0984

GA_{OTs}: Compound **4** (29 mg, 0.04 mmol), trimethylamine solution in EtOH (20%) (0.6 mL) and DCM (0.6 mL) were mixed in a Schlenk tube under N_2 condition. The Schlenk tube was sealed and heated at 50 °C for 16 h. After the reaction completed, the mixture was evaporated under vacuum. The resulting residue was dissolved by a solvent mixture of DCM/MeOH (10/1) and subjected to flash column chromatography (DCM/MeOH = 10/1, R_f = 0.3) to afford a crude product. The crude product was then washed by a solvent mixture of EA/DCM/MeOH (200/200/1, 1.0 mL) for three times, obtaining purified **GA_{OTs}** as a yellow solid (14.5 mg, 0.018 mmol, 46% yield). ^{1}H NMR (400 MHz, CD_3OD) δ 9.49 (d, J = 6.1 Hz, 1H), 8.24 – 8.15 (m, 1H), 8.00 (d, J = 8.2 Hz, 1H), 7.69 (d, J = 8.7 Hz, 1H), 7.54 – 7.45 (m, 1H), 7.37 (d, J = 2.5 Hz, 1H), 6.93 (dd, J = 8.6, 2.4 Hz, 1H), 4.08 (t, J = 6.4 Hz, 2H), 3.38 – 3.31 (m, 2H), 3.13 (s, 9H), 1.88 – 1.73 (m, 4H), 1.58 – 1.46 (m, 2H), 1.47 – 1.34 (m, 8H). ^{13}C NMR (101 MHz, CD_3OD) δ 164.7, 160.3, 153.2, 147.6, 143.2, 134.2, 127.5, 123.0, 120.9, 116.0, 114.9, 68.2, 66.5, 52.1, 28.9, 28.8, 28.7, 28.5, 25.9, 25.5, 22.6. HR-MS (ESI+) calculated for $C_{23}H_{34}AuCl_2N_2O$ $[M–OTs]^+$ 621.1714 found 621.1712.

Compound 5: 2-(4-Hydroxyphenyl)pyridine (1.71 g, 10.0 mmol) and NaOH (400 mg, 10.0 mmol) were dissolved in ethanol (20 mL), which was added dropwise into a solution of 1,9-dibromononane (2.86 g, 10.0 mmol) in ethanol (20 mL) at 80 °C under N_2 condition. The mixture was heated and stirred at 80 °C under N_2 for 16 h. When the reaction completed, the resulting mixture was concentrated by rotary evaporation and subjected to column chromatography (*n*-hexane/EA = 5/1, R_f = 0.4) to obtain product **5** as a white solid (1.50 g, 4.0 mmol, 40% yield). ^{1}H NMR (400 MHz, $CDCl_3$) δ 8.64 (d, J = 4.8 Hz, 1H), 7.98 – 7.90 (m, 2H), 7.74 – 7.63 (m, 2H), 7.19 – 7.12 (m, 1H), 6.98 (d, J = 8.8 Hz, 2H), 4.01 (t, J = 6.5 Hz, 2H), 3.41 (t, J = 6.9 Hz, 2H), 1.91 – 1.74 (m, 4H), 1.52 – 1.40 (m, 4H), 1.40 – 1.29 (m, 6H). ^{13}C NMR (101 MHz, $CDCl_3$) δ 160.0, 157.2, 149.5, 136.6, 131.8, 128.1, 121.3, 119.8, 114.7, 68.0, 34.0, 32.8, 29.4, 29.3, 29.2, 28.7, 28.2, 26.0. HR-MS (ESI+) calculated for $C_{20}H_{26}BrNO$ $[M+H]^+$ 376.1271 found 376.1284.

Compound 6: Compound **5** (1.2 g, 3.2 mmol) and $Hg(OAc)_2$ (1.1 g, 3.5 mmol) were suspended in dioxane (40 mL) and heated at 100 °C for 24 h. Then, LiCl (297 mg, 7.0 mmol) was added to the mixture, and heated at 100 °C for further 1 h. After the reaction completed, the mixture was concentrated by rotary evaporation and subjected to flash column chromatography (*n*-Hexane/DCM = 2/1, R_f = 0.5) to afford compound **6** as a white solid (747 mg, 1.22 mmol, 38% yield). ^{1}H NMR (400 MHz, $CDCl_3$) δ 8.56 (d, J = 4.5 Hz, 1H), 7.95 (d, J = 8.7 Hz, 1H), 7.86 (d, J = 8.1 Hz, 1H), 7.81 – 7.72 (m, 1H), 7.33 – 7.26 (m, 1H), 7.08 (d, J = 2.7 Hz, 1H), 6.90 (dd, J = 8.7, 2.8 Hz, 1H), 4.01 (t, J = 6.5 Hz, 2H), 3.41 (t, J = 6.8 Hz, 2H), 1.92 – 1.75 (m, 4H), 1.53 – 1.40 (m, 4H), 1.40 – 1.26 (m, 6H). ^{13}C NMR (101 MHz, $CDCl_3$) δ 160.2, 155.4, 147.8, 138.1, 133.9, 127.8, 123.6, 122.6, 119.6, 114.8, 68.2, 34.1, 32.8, 29.4, 29.3, 29.2, 28.7, 28.2, 26.0. HR-MS (ESI+) calculated for $C_{20}H_{25}BrClHgNO$ $[M+H]^+$ 612.0570 found 612.0558.

Compound 7: Compound **7** was synthesized according to a published method.[44] Compound **6** (735 mg, 1.20 mmol) and $KAuCl_4{\cdot}2H_2O$ (662 mg, 1.6 mmol) were dissolved in a solvent mixture of ACN/DCM (1/1, total 10 mL) and heated at 50 °C for 16 h. Then, the solution was concentrated by rotary evaporation. The resulting residue was suspended by DCM (200 mL), filtered and washed by DCM (50 mL) to obtain the purified product of compound **7** as a yellow solid (0.62 g, 0.96 mmol, 80% yield). ^{1}H NMR

(400 MHz, $CDCl_3$) δ 9.70 (d, J = 6.2 Hz, 1H), 8.08 – 8.01 (m, 1H), 7.72 (d, J = 8.1 Hz, 1H), 7.60 (d, J = 2.5 Hz, 1H), 7.48 (d, J = 8.6 Hz, 1H), 7.40 – 7.34 (m, 1H), 6.90 (dd, J = 8.6, 2.4 Hz, 1H), 4.07 (t, J = 6.5 Hz, 2H), 3.42 (t, J = 6.8 Hz, 2H), 1.92 – 1.75 (m, 4H), 1.51 – 1.41 (m, 4H), 1.40 – 1.29 (m, 6H). Due to the low solubility, ^{13}C NMR spectrum of compound **7** cannot be obtained. HR-MS (ESI+) calculated for $C_{20}H_{25}AuBrCl_2NO$ $[M+Na]^+$ 664.0054 found 664.0048.

GA_{Br}: Compound **7** (14 mg, 0.022 mmol), trimethylamine solution in EtOH (20%) (0.5 mL) and DCM (0.5 mL) were mixed in a Schlenk tube under N_2 condition. The Schlenk tube was sealed and heated at 50 °C for 16 h. After the reaction completed, the mixture was evaporated under vacuum. The resulting residue was dissolved by a solvent mixture of DCM/MeOH (10/1) and subjected to flash column chromatography (DCM/MeOH = 10/1, R_f = 0.3) to afford a crude product. The crude product was then washed by a solvent mixture of EA/DCM/MeOH (200/200/1, 1.0 mL) for three times, obtaining purified **GA_{Br}** as a yellow solid (4.0 mg, 0.0057 mmol, 26% yield). ^1H NMR (400 MHz, CD_3OD) δ 9.48 (d, J = 5.3 Hz, 1H), 8.22 – 8.15 (m, 1H), 7.99 (d, J = 7.3 Hz, 1H), 7.67 (d, J = 8.6 Hz, 1H), 7.52 – 7.45 (m, 1H), 7.34 (d, J = 2.4 Hz, 1H), 6.91 (dd, J = 8.6, 2.4 Hz, 1H), 4.07 (t, J = 6.5 Hz, 2H), 3.38 – 3.32 (m, 2H), 1.86 – 1.76 (m, 4H), 1.57 – 1.49 (m, 2H), 1.49 – 1.36 (m, 8H). ^{13}C NMR (101 MHz, CD_3OD) δ 164.8, 160.3, 153.2, 147.6, 143.2, 134.3, 127.4, 123.0, 120.8, 116.0, 114.9, 68.2, 66.5, 52.1, 28.9, 28.7, 28.7, 28.5, 25.9, 25.5, 22.6. HR-MS (ESI+) calculated for $C_{23}H_{34}AuCl_2N_2O$ $[M–Br]^+$ 621.1714 found 621.1710.

Acknowledgements

We gratefully acknowledge financial support of this work by the Hong Kong Research Grants Council, General Research Fund (GRF 15300520 to M.K.W.), Early Career Scheme (ECS 25301320 to F.K.C.L.), the Croucher Foundation (Croucher Innovation Award-2021 to F.K.C.L.), The Hong Kong Polytechnic University Start-up Fund (1-BE2H to F.K.C.L.), and Dean's Reserve (P0034752 to M.K.W. and F.K.C.L).

Conflict of Interest

The authors declare no conflict of interest.

Keywords: Aqueous Media • Controlled Assembly • Gold (III) Complex • Molecular Amphiphile • Supramolecular Assembly

Reference

[1] N. S. Simmons, E. R. Blout, *Biophys. J.* **1960**, *1*, 55–62.
[2] T. Lino, *J. Supramol. Struct.* **1974**, *2*, 372–384.
[3] D. Chapman, *Q. Rev. Biophys.* **1975**, *8*, 185–235.
[4] S. Chen, R. Costil, F. K. C. Leung, B. L. Feringa, *Angew. Chem. Int. Ed.* **2021**, *60*, 11604–11627.
[5] E. Krieg, M. M. C. Bastings, P. Besenius, B. Rybtchinski, *Chem. Rev.* **2016**, *116*, 2414–2477.
[6] B. L. Feringa, *Angew. Chem. Int. Ed.* **2017**, *56*, 11060–11078.
[7] T. Aida, E. W. Meijer, S. I. Stupp, *Science* **2012**, *335*, 813–817.
[8] D. Dattler, G. Fuks, J. Heiser, E. Moulin, A. Perrot, X. Yao, N. Giuseppone, *Chem. Rev.* **2020**, *120*, 310–433.
[9] M. Baroncini, S. Silvi, A. Credi, *Chem. Rev.* **2020**, *120*, 200–268.
[10] H. Shigemitsu, T. Fujisaku, W. Tanaka, R. Kubota, S. Minami, K. Urayama, I. Hamachi, *Nat. Nanotechnol.* **2018**, *13*, 165–172.
[11] J. Volarić, W. Szymanski, N. A. Simeth, B. L. Feringa, *Chem. Soc. Rev.* **2021**, *50*, 12377–12449.
[12] J. K. L. Poon, Z. Chen, S. Y. L. Leung, M. Y. Leung, V. W. W. Yam, *Proc. Natl. Acad. Sci. U. S. A.* **2021**, *118*, 1–9.
[13] V. W. W. Yam, A. S. Y. Law, *J. Chinese Chem. Soc.* **2020**, *67*, 2246–2252.
[14] H. L. K. Fu, V. W. W. Yam, *Chem. Lett.* **2018**, *47*, 605–610.
[15] T. Owen, A. Butler, *Coord. Chem. Rev.* **2011**, *255*, 678–687.
[16] M. J. Mayoral Muñoz, G. Fernández, *Chem. Sci.* **2012**, *3*, 1395–1398.
[17] W. Zi, F. Dean Toste, *Chem. Soc. Rev.* **2016**, *45*, 4567–4589.
[18] J. J. Jiang, M. K. Wong, *Chem. Asian J.* **2021**, *16*, 364–377.
[19] L. Rocchigiani, M. Bochmann, *Chem. Rev.* **2021**, *121*, 8364–8451.
[20] V. W. W. Yam, A. K. W. Chan, E. Y. H. Hong, *Nat. Rev. Chem.* **2020**, *4*, 528–541.
[21] V. W. W. Yam, V. K. M. Au, S. Y. L. Leung, *Chem. Rev.* **2015**, *115*, 7589–7728.
[22] P. Destito, C. Vidal, F. López, J. L. Mascareñas, *Chem. - Eur. J.* **2021**, *27*, 4789–4816.
[23] S. R. Thomas, A. Casini, *Curr. Opin. Chem. Biol.* **2020**, *55*, 103–110.
[24] T. C. Chang, K. Tanaka, *Bioorganic Med. Chem.* **2021**, *46*, 116353.
[25] J. J. Zhang, W. Lu, R. W. Y. Sun, C. M. Che, *Angew. Chem. Int. Ed.* **2012**, *51*, 4882–4886.
[26] V. K. M. Au, N. Zhu, V. W. W. Yam, *Inorg. Chem.* **2013**, *52*, 558–567.
[27] K. C. Yim, E. S. H. Lam, K. M. C. Wong, V. K. M. Au, C. C. Ko, W. H. Lam, V. W. W. Yam, *Chem. - A Eur. J.* **2014**, *20*, 9930–9939.
[28] S. K. L. Siu, C. Po, K. C. Yim, V. K. M. Au, V. W. W. Yam, *CrystEngComm* **2015**, *17*, 8153–8162.
[29] K. C. Yim, V. K. M. Au, L. L. Hung, K. M. C. Wong, V. W. W. Yam, *Chem. - A Eur. J.* **2016**, *22*, 16258–16270.
[30] F. Wang, M. Lan, W. P. To, K. Li, C. N. Lok, P. Wang, C. M. Che, *Chem. Commun.* **2016**, *52*, 13273–13276.
[31] B. Kemper, L. Zengerling, D. Spitzer, R. Otter, T. Bauer, P. Besenius, *J. Am. Chem. Soc.* **2018**, *140*, 534–537.
[32] Q. Wan, J. Xia, W. Lu, J. Yang, C. M. Che, *J. Am. Chem. Soc.* **2019**, *141*, 11572–11582.
[33] M. Y. Leung, S. Y. L. Leung, K. C. Yim, A. K. W. Chan, M. Ng, V. W. W. Yam, *J. Am. Chem. Soc.* **2019**, *141*, 19466–19478.
[34] J. J. Jiang, J. F. Cui, B. Yang, Y. Ning, N. C. H. Lai, M. K. Wong, *Org. Lett.* **2019**, *21*, 6289–6294.
[35] J. F. Cui, H. M. Ko, K. P. Shing, J. R. Deng, N. C. H. Lai, M. K. Wong, *Angew. Chem. Int. Ed.* **2017**, *56*, 3074–3079.
[36] H. Y. Sit, B. Yang, K. Ka-Yan Kung, J. Siu-Lun Tam, M. K. Wong, *Chempluschem* **2019**, *84*, 1739–1743.
[37] K. K. Y. Kung, H. M. Ko, J. F. Cui, H. C. Chong, Y. C. Leung, M. K. Wong, *Chem. Commun.* **2014**, *50*, 11899–11902.
[38] H. M. Ko, J. R. Deng, J. F. Cui, K. K. Y. Kung, Y. C. Leung, M. K. Wong, *Bioorganic Med. Chem.* **2020**, *28*, 115375.
[39] S. Chen, F. K. C. Leung, M. C. A. Stuart, C. Wang, B. L. Feringa, *J. Am. Chem. Soc.* **2020**, *142*, 10163–10172.
[40] F. K.-C. Leung, C. A. Marc, T. Kajitani, T. Fukushima, B. L. Feringa, *Angew. Chem. Int. Ed.* **2019**, *58*, 10985–10989.
[41] J. Chen, F. K. C. Leung, M. C. A. Stuart, T. Kajitani, T. Fukushima, E. Van Der Giessen, B. L. Feringa, *Nat. Chem.* **2018**, *10*, 132–138.
[42] S. Liu, Y. I. González, D. Danino, E. W. Kaler, *Macromolecules* **2005**, *38*, 2482–2491.
[43] E. C. Constable, T. A. Leese, *J. Organomet. Chem.* **1987**, *335*, 293–299.
[44] E. C. Constable, T. A. Leese, *J. Organomet. Chem.* **1989**, *363*, 419–424.

Man-Kin Wong

Man-Kin Wong obtained his BSc in Chemistry from The University of Hong Kong (HKU), where he carried out his PhD with research focus on catalytic asymmetric epoxidation under the supervision of Prof. Dan Yang. In 1999, after his postdoc training, he was serving as a research assistant professor of Prof. Chi-Ming Che's team in HKU. Since 2008, he joined in Department of Applied Biology and Chemical Technology, The Hong Kong Polytechnic University. Currently, he is serving as an associate professor and associate head of the department. His main research interests are gold(III) organometallic chemistry and asymmetric catalysis, chemical biology, as well as photocatalysis.

Franco King-Chi Leung

Franco King-Chi Leung studied his BSc in Chemistry at The Hong Kong Polytechnic University where he carried out his master's research in catalysis and chemical biology under the supervision of Prof. Man Kin Wong. He expanded his research scopes in his PhD to supramolecular chemistry and material science under the guidance of Prof. Takanori Fukushima in Tokyo Institute of Technology (Japan). In 2017, he joined Prof. Ben L. Feringa's group (2016 Nobel Laureate in Chemistry), as a postdoc fellow and later he was awarded the Croucher Postdoctoral Fellow, where he has developed responsive supramolecular systems. In 2019, he was appointed as assistant professor in Department of Applied Biology and Chemical Technology, The Hong Kong Polytechnic University. His main research interests are photoresponsive molecular amphiphiles, dynamic supramolecular polymers, functional molecular assembly, and biocompatible functional materials.

Table of Contents

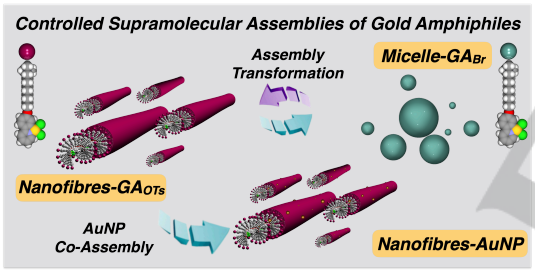

Controlled supramolecular transformation of gold (III) amphiphiles are responsive to external stimulations. We provide a study of counterion exchange to supramolecular structural transformation of gold (III) amphiphiles and their co-assembly with gold nanoparticles.